

Analysis of FDTD Field Simulation and Experimental Results in a Monopole Antenna Array Coil at 7T

Myung-Kyun Woo¹, Suk-Min Hong², Jongho Lee¹, Young-Bo Kim³, and Zang-Hee Cho⁴

¹Department of Electrical and Computer Engineering, Seoul National University, Seoul, Korea, ²Institute of Neuroscience and Medicine - 4, Forschungszentrum Jülich, Jülich, Germany, ³Gil Hospital, Incheon, Korea, ⁴Neuroscience Research Institute, Incheon, Korea

INTRODUCTION: One of the primary challenges at an Ultra-high field (UHF) MRI system is B_1^+ field non-uniformity. To overcome this challenge, a number of RF coils have been developed. Recently, radiative antennas have been proposed (1) as an approach to improve the uniformity. A Monopole antenna Array (MA) coil, a type of radiative antennas, demonstrated to have a relatively uniform coverage in transverse plane (2). However, the coil showed limited coverage along z-direction. To overcome this limitation, an improved version of this coil, Extended Monopole antenna Array with individual shields (EMAS) coil, was proposed (3). This coil successfully extended the coverage of the coil up to cerebellum and may potentially be useful in clinical applications at UHF. In this work, the performance of EMAS coil was evaluated by using FDTD field simulation and experiment results. Additionally, specific absorption rate (SAR) was calculated using the simulation and compared the results with the other coils (MA and Extended Monopole antenna Array with no shields (EMA)).

METHODS: Computational electromagnetic simulation (xFDTD; REMCOM, State College, PA) was performed for B_1^+ field and SAR. Three eight-channel coils, MA, EMA and, EMAS coils, were simulated and driven by one voltage source for each channel with identical amplitude. Active voltage sources were placed between the monopole and ground plate. Each channel had a 45° phase shift in order to generate a uniform birdcage-like mode. A high-fidelity head model that includes shoulders was selected for the geometry with a 2 x 2 x 2 mm³ resolution. The average SAR and maximum SAR_{10g} values were calculated based on a 90° pulse (3 ms) marked in Figure 2a (white crosshairs). The point for calculation was 2 x 2 mm². To compare the simulation results with experimental results, a flip angle map was acquired in all three coils using an actual flip angle imaging (AFI) pulse sequence (TR1/TR2 = 20/100 ms). High resolution T₂^{*}-weighted gradient echo (GRE) images (TR = 750 ms, TE = 18ms, voxel size = 0.25 x 0.25 x 2 mm³) were acquired and proton density-weighted images (TR = 1000 ms, TE = 2.5 ms) were obtained to investigate the SNR of each coil. For a quantitative comparison, multiple ROIs (3 x 3 cm²) were chosen at the sagittal (6 ROIs), coronal (5 ROIs), and axial planes (6 ROIs) at approximately the same locations in both simulation and experiment.

RESULTS: Figure 1 shows the simulated B_1^+ maps (Fig. 1a) and the measured flip angle maps (Fig. 2b) for each coil in the sagittal, coronal, and axial planes. In the sagittal plane, the mean ROI values of the simulated B_1^+ were similar in all three coils. For the axial planes, however, the mean ROI values showed 40% difference between EMAS and MA (and EMA) coils. Similar field patterns were observed at the measured flip angle maps showing a large difference (46.1%) between EMAS and MA coils in the axial plane. Average SAR and maximum SAR_{10g} (W/kg) for the MA, EMA, and EMAS coils are listed in Table 1. The three coils showed similar average SARs. However, maximum SAR_{10g} for EMAS coil were smaller than the other coils. This may indicate that electric field distribution of the EMAS coil was relatively uniform. Figure 2 shows high resolution T₂^{*}-weighted GRE images and SNR maps for the three coils. These results show that the EMAS coil clearly demonstrates extended spatial coverage compared to the MA and EMA coils.

DISCUSSION and CONCLUSION: The computer simulation results suggest a good agreement with the experiment results. The images from the EMAS coil clearly demonstrates extended spatial coverage compared to the MA and EMA coils. The EMAS coil improves B_1^+ field at the inferior part of the brains and, therefore, may be applicable in various clinical applications.

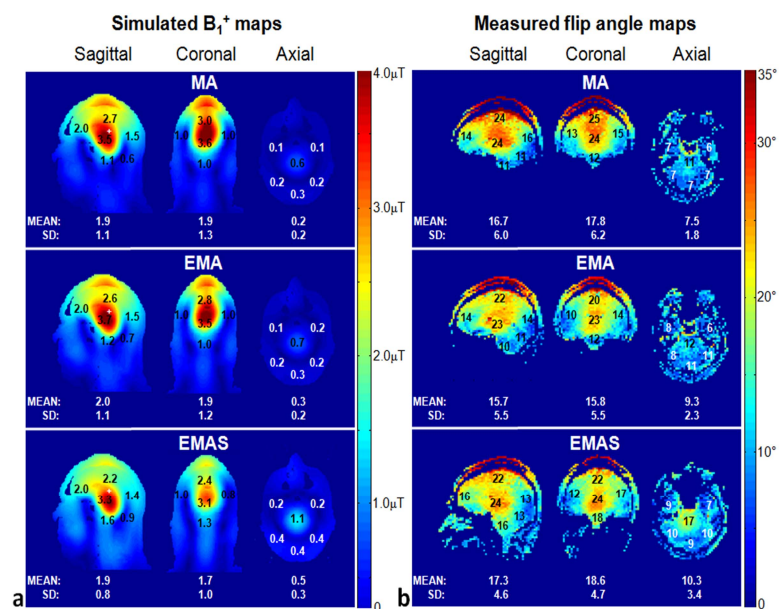


Fig. 1. (a) Simulated B_1^+ maps (in μT) and (b) measured flip angle maps (in degrees) in the sagittal, coronal and axial planes.

Figure 2 shows high resolution T₂^{*}-weighted GRE images and SNR maps for the three coils. The figure includes three panels: (a) MA, (b) EMA, and (c) EMAS. Each panel shows a grayscale brain image with a white crosshair indicating the ROI, followed by a color-coded SNR map. Numerical values for mean and standard deviation are provided for each panel.

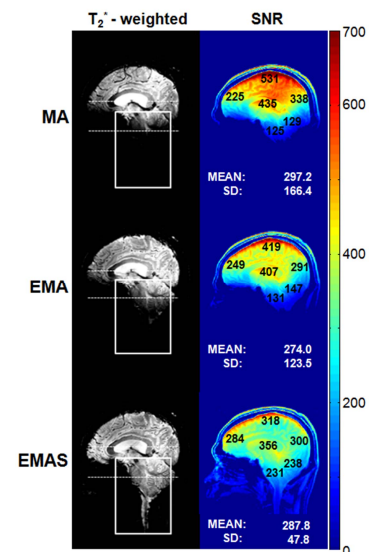


Fig. 2. High resolution T₂^{*}-weighted GRE images and SNR maps acquired with the (a) MA, (b) EMA, and (c) EMAS coils, respectively.

Table 1. Average SAR and maximum SAR_{10g} values of the simulated B_1^+ when the reference point for the RF pulse was at the white cross hairs in Figure 1a.

Reference RF point	Coil	SAR Average (W/kg)	SAR Max. 10g (W/kg)
Isocenter (at the cross hairs in Figure 2a)	MA	1.2	5.8
	EMA	1.2	5.9
	EMAS	1.1	4.8

REFERENCE: [1] A. J. E. Raaijmakers et. al., MRM, 66, 5 (2011) [2] SM Hong et. al., MRM, 71, 5 (2014) [3] MK Woo et.al., ISMRM 2014, Milano, p 401